nature photonics

SUPPLEMENTARY INFORMATION

DOI: 10.1038/NPHOTON.2014.177

Non-reciprocal phase shift induced by an effective magnetic flux for light

Lawrence D. Tzuang,[1] Kejie Fang,[2,3] Paulo Nussenzveig,[1,4] Shanhui Fan,[2] and Michal Lipson[1,5]

[1]*School of Electrical and Computer Engineering, Cornell University,*

Ithaca, New York 14853, USA.

[2]*Department of Electrical Engineering, Stanford University, Stanford,*

California 94305, USA

3Thomas J. Watson, Sr., Laboratory of Applied Physics, California Institute of Technology,

Pasadena, CA 91125, USA

[4]*Instituto de Física, Universidade de São Paulo, P.O. Box 66318,*

05315-970 São Paulo, Brazil

[5]*Kavli Institute at Cornell for Nanoscale Science, Cornell University,*

Ithaca, New York 14853, USA

(Dated: June 23, 2014)

DOI: 10.1038/NPHOTON.2014.177

Frequency separation of Photonic two-level system in a silicon coupled-waveguides structure

The frequency separation between the even and the odd-mode can be controlled through engineering the geometry of the coupled-waveguide shown in Fig. 2e. For example, by designing a smaller gap width, the frequency separation between the two modes (Δf) becomes larger, and vice versa as shown in Fig. S1a. In the ideal case, Δf should match the RF modulation frequency (f_M). However, the frequency separation of the two modes is not constant across wavelength because their dispersion curves (solid, blue and red) are not in parallel as shown in Fig. S1b.

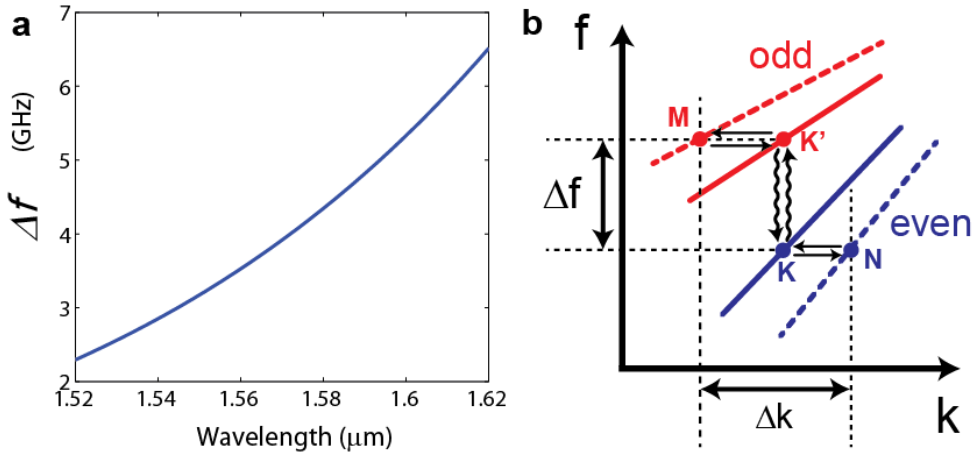

Fig. S1: **Dispersion relation of the even and odd modes in a silicon coupled-waveguides structure.** (a) Simulation of the frequency separation of even- and odd-mode for the waveguide geometry defined in Fig. 2a. (b) A depiction of the dispersion curves for both even (blue) and odd (red) modes at the RF modulation regions (solid) and at the middle modulation-free region (dashed). The modulation frequency f_M ideally should match the frequency separation between the two modes Δf.

Transfer matrices for a photonic Ramsey-type interferometer with perfect phase-matching

Sinusoid RF signals are applied to a photonic Ramsey-type interferometer to induce coupling between the even- and the odd-mode in a silicon coupled-waveguide structure. This coupling will also impart an extra phase shift on light originating from the RF phase. This is described through the coupled mode equations[1-3]:

$$i\frac{d}{dt}\begin{pmatrix} a_1 \\ a_2 \end{pmatrix} = \begin{pmatrix} 0 & \kappa e^{-i\phi_{L(R)}} \\ \kappa^* e^{i\phi_{L(R)}} & 0 \end{pmatrix}\begin{pmatrix} a_1 \\ a_2 \end{pmatrix}, \qquad (1)$$

where $a_{1(2)}$ are the amplitude of the mode, κ is the coupling rate between the two modes, and $\phi_{L(R)}$ is the RF phase of the left (right) modulator. From Eq. (1), we see that coupling from mode 1 to mode 2 acquires a $-\phi$ phase, whereas the transition from mode 2 back to mode 1 acquires $+\phi$ phase. Eq. (1) also assumes perfect phase-matching (i.e., $f_M = \Delta f$), and $\kappa << f_M$. Following Eq. (1), the transfer matrix of the modulator can be written as:

$$T_{L(R)} = \begin{pmatrix} \cos(\kappa \cdot t) & ie^{-i\phi_{R(L)}} \sin(\kappa \cdot t) \\ ie^{i\phi_{L(R)}} \sin(\kappa \cdot t) & \cos(\kappa \cdot t) \end{pmatrix}, \qquad (2)$$

where t is the time lapse of light propagating in the RF modulation region. Ideally in a photonic Ramsey-type interferometer, we design the length of the electrode such that $t = \pi/(4\kappa)$ which provides a 50 % transition between the two photonic states.

In the middle modulation-free region, light in each of the photonic states experiences different amount of phase shift ϕ_1 and ϕ_2 because of the gap tapering of the coupled-waveguides. This effect is illustrated in Fig. S1b, where the tapering of the coupled-waveguide gap forces light in the original two photonic states (K and K' with the same k vector and separated by f_M) to propagate into new photonics states (M and N) with their k-vectors separated by $\Delta k(\lambda)$. After light in both photonic states travel for a distance L_f (Fig. 2e), the phase difference acquired by the two photonic states becomes $L_f\Delta k = \phi_1 - \phi_2$, and the transfer matrix can be written as:

DOI: 10.1038/NPHOTON.2014.177

$$T_f = \begin{pmatrix} e^{i\phi_1} & 0 \\ 0 & e^{i\phi_2} \end{pmatrix}. \qquad (3)$$

The final transfer matrix for the photonic Ramsey-type interferometer can be obtained by cascading Eqs. (2) and (3):

$$T_{L\to R} = T_R T_f T_L = \frac{1}{2}\begin{pmatrix} e^{i\phi_1} - e^{i(\phi_2+\phi_L-\phi_R)} & ie^{i(\phi_1-\phi_L)} + ie^{i(\phi_2-\phi_R)} \\ ie^{i(\phi_2+\phi_L)} + ie^{i(\phi_1+\phi_R)} & e^{i\phi_2} - e^{i(\phi_1+\phi_R-\phi_L)} \end{pmatrix}. \qquad (4)$$

$$T_{R\to L} = T_L T_f T_R = \frac{1}{2}\begin{pmatrix} e^{i\phi_1} - e^{i(\phi_2+\phi_R-\phi_L)} & ie^{i(\phi_1-\phi_R)} + ie^{i(\phi_2-\phi_L)} \\ ie^{i(\phi_2+\phi_R)} + ie^{i(\phi_1+\phi_L)} & e^{i\phi_2} - e^{i(\phi_1+\phi_L-\phi_R)} \end{pmatrix}. \qquad (5)$$

In Eqs. (4) and (5), we have assumed the ideal case where $t = \pi/(4C)$.

Transfer matrices for a photonic Ramsey-type interferometer with phase detuning

If $\Delta f \neq f_M$, the perfect phase-matching condition for the coupling between the two modes is broken, and we have to rewrite Eq. (5) using its general form[4]:

$$T_{L(R)} = \begin{pmatrix} \cos(C\cdot t) + i\frac{\Delta}{2C}\sin(C\cdot t) & i\frac{\kappa}{C}e^{-i\phi_{R(L)}}\sin(C\cdot t) \\ i\frac{\kappa}{C}e^{i\phi_{L(R)}}\sin(C\cdot t) & \cos(C\cdot t) - i\frac{\Delta}{2C}\sin(C\cdot t) \end{pmatrix}, \qquad (6)$$

where $\Delta = 2\pi(f_M - \Delta f)$, C is the Rabi oscillation frequency (i.e., $C = \sqrt{\kappa^2 + \Delta^2}$). In Eq. (6), we have also assume that $C << 2\pi(f_M)$.

Simulation of the fringe phases versus L_f

Measuring the fringe phase difference between the two propagation directions ($\phi_{L\rightarrow R}$ - $\phi_{R\rightarrow L}$) allows us to identify the phase difference accumulated by the two photonic modes ($\Delta\phi_p$) in the tapered-region. Here we assume $\Delta\phi_p$ is solely contributed from the tapered-region L_f. From Eqs. (4) and (5), the forward and backward transmissions versus $\Delta\phi_p$ are sinusoidal functions (fringes) with their phase difference expressed as:

$$\phi_{L\rightarrow R} - \phi_{R\rightarrow L} = 2\Delta\phi_p = 2\gamma(\Delta k)L_f, \quad (7)$$

where Δk is obtained directly from COMSOL by solving the effective indices of both the even- and odd-mode at the tapered-region. In Eq. (7), γ accounts for the extra phase acquired in L_f because of the presence of a Fabry-Perot (FP)[4]:

$$\gamma = 2B, \quad (8)$$

where B = (1 / (*2-R-R*)) is the effective round trip number inside the FP cavity. This FP cavity is formed in between the two tapers due to the change in waveguide geometry. The reflection coefficient R of these tapers can be obtained from the transmission spectrum (without applying RF signal) using the expression[4]:

$$T = T_{in}\frac{(1-R)^2}{\left|1-R\cdot e^{2jkL_f}\right|}, \quad (9)$$

where T and T_{in} is the output and input optical power, and k is the wavevector. Here we show the transmission spectrum for L_f = 350 μm is shown in Fig. S2. From the curve fitting we obtain the reflection R of 0.18 and a cavity finesse of 2.5. We can therefore use Eq. (8) and obtain γ = 1.24.

DOI: 10.1038/NPHOTON.2014.177

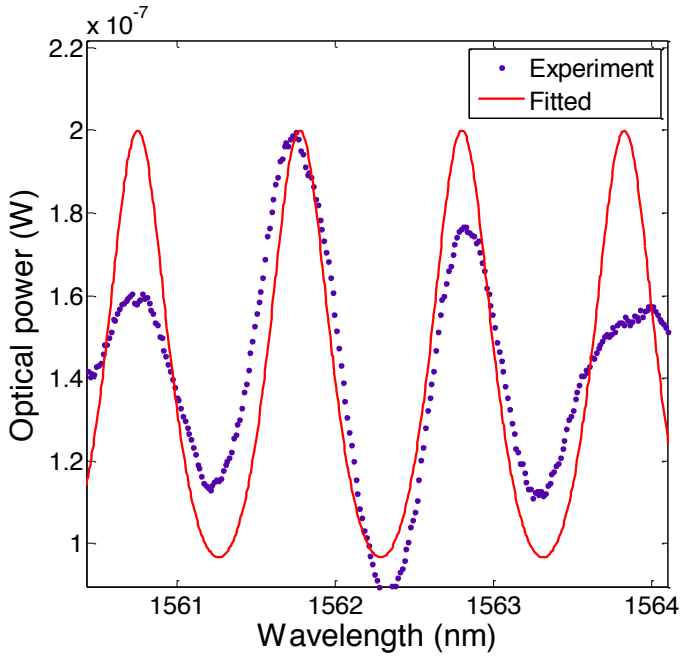

Fig. S2: **Measurement of the optical transmission spectrum.** Measured (dotted, blue) and fitted (solid, red) transmission spectrum for $L_f = 350$ μm.

Testing setup

The experimental setup is shown in Fig. S3. Details of the measurement can be found in Methods section in the main article.

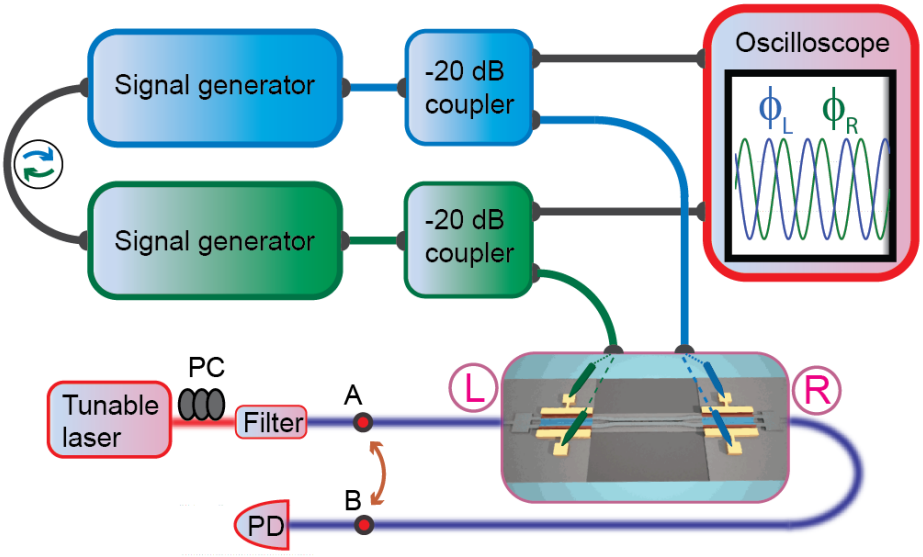

Fig. S3: **Experimental setup that measures the non-reciprocity and the interference fringes for the photonic Ramsey-type interferometer.** The two signal generators are synchronized to ensure correlated phase between the two RF signals, and these signals are monitored through the oscilloscope. Fibers connecting to point A and B from the laser and photodetector (PD) ends are interchangeable to measure forward and backward light transmission.

The RC bandwidth of our photonic Ramsey interferometer

Because of the long modulation length (3.8 mm), our device bandwidth is 2.5 GHz that undermines our modulation efficiency. This number is estimated by the measured capacitance and resistance. The capacitance includes both the electrode capacitance and the diode capacitance (~0.27 fF/μm). This measured capacitance matches our SILVACO simulation of ~ 0.25 fF/μm. The resistance is mainly dominated by the 50 Ω system. Based on these numbers, the voltage RC response can be calculated as shown in Fig. S4.

DOI: 10.1038/NPHOTON.2014.177

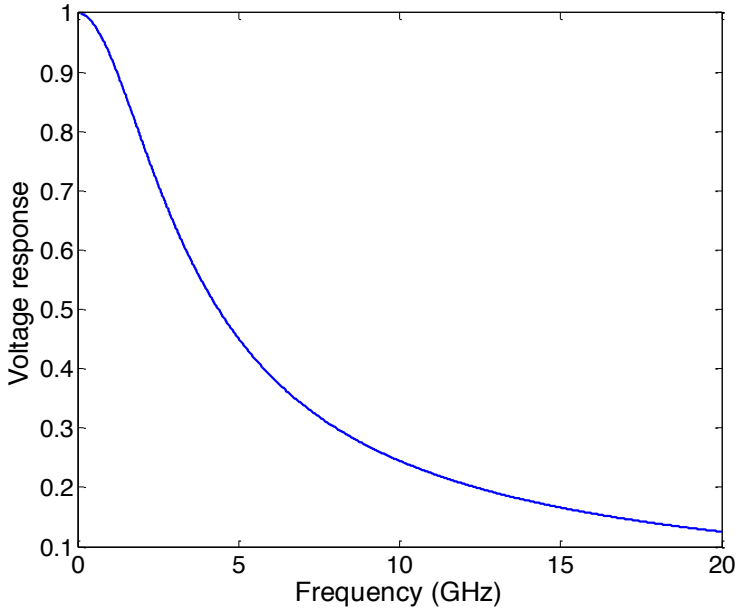

Fig. S4: **Estimated voltage response for our interferometer.** Calculated voltage with an input voltage of 1 V at different RF frequencies based on the measured capacitance of our devices.

Theoretical RF power for maximum fringe extinction ratio

The maximum fringe extinction ratio is obtained when both modulators provide an equal population probability (i.e. 50 %) of photons in both the even- and the odd- modes. As shown in Fig. S5a, this condition requires that the coupling strength in the spatial domain $C_s = C_0 = (\pi/(4L_m))$, where L_m is the length of the modulator. Decreasing C_s will result in a smaller fringe extinction ratio. In our experiments, $L_m = 3.9$ mm, therefore $C_0 = 200$ 1/m. As shown in Fig. S5b, we show the theoretical C_s as a function of applied voltage. From this figure, $C_s = C_0$ is met at a peak voltage of 4 V, which corresponds to a RF power of $P_0 = 160$ mW in a 50 Ω system. Since the device is operated in the RC cut-off regime (as shown in Fig. S4), the extrapolated RF power (at 4 GHz) for maximum extinction ratio ($P_{0,extract}$) becomes 570 mW (27.5 dBm).

The coupling strength C_s is proportional to the dielectric constant modulation, which is also proportional to the RF peak voltage (V). Therefore, the relation between C and the RF power (P_{RF}) can be obtained as:

$$C_s \propto \Delta\varepsilon \propto \sqrt{V} \propto (P_{RF})^{1/4}, \qquad (10)$$

where Δε is the dielectric constant shift. The square root voltage relation is the signature of the diode.

Our experimental results shown in Fig. 3c indicates that a 34 dBm RF power is not enough (around 42 % extinction ratio) to obtain the maximum extinction ratio. This can be caused by the imperfections in the pn diodes (the diode profile is not perfectly fabricated resulting from misalignment in our e-beam lithography). Based on the results shown in figures 3, S4, S5a, and S5b, we estimate our diode provides about 28 % of the designed diode efficiency (Fig. S5b).

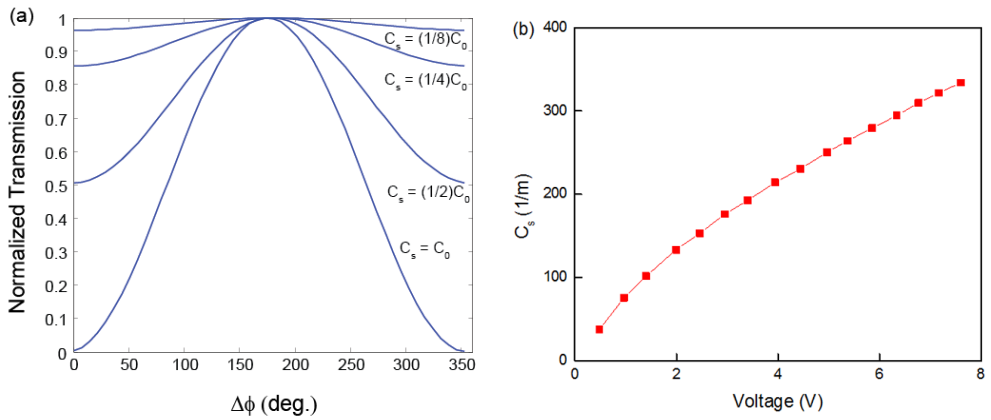

Fig. S5: **Theoretical interference fringe for different coupling strength and the theoretical coupling strength versus voltage.** (a) The fringes increase in extinction ratio as the coupling strength (C) is increased, where C_0 is the optimum coupling strength when the even- and odd-modes are equally populated. (b) The coupling strength increases as the applied peak voltage increases.

DOI: 10.1038/NPHOTON.2014.177

Testing setup with an RF amplifier

In Fig. 3c (fringes for different RF powers), we apply high RF powers that exceeds the maximum output power from the signal generator (at 24 dBm) by using an RF amplifier. This particular experimental setup is shown in Fig. S6. The sinusoidal RF wave from the signal generator is amplified through an RF amplifier. Then, the wave splits into two RF arms and applied to the device through a pair of RF probes. We drop -20 dB of power from each RF arm to monitor their phases. A phase shifter is added to one RF arm to control the phase difference between the two arms. The optical part of the setup is identical to Fig. S3. The maximum RF power we obtain for each RF arm is about 34 dBm. Based on Eq. (10), the 34 dBm maximum power corresponds to a factor of 1.8 increase of the coupling strength compared to the maximum power directly from the signal generator.

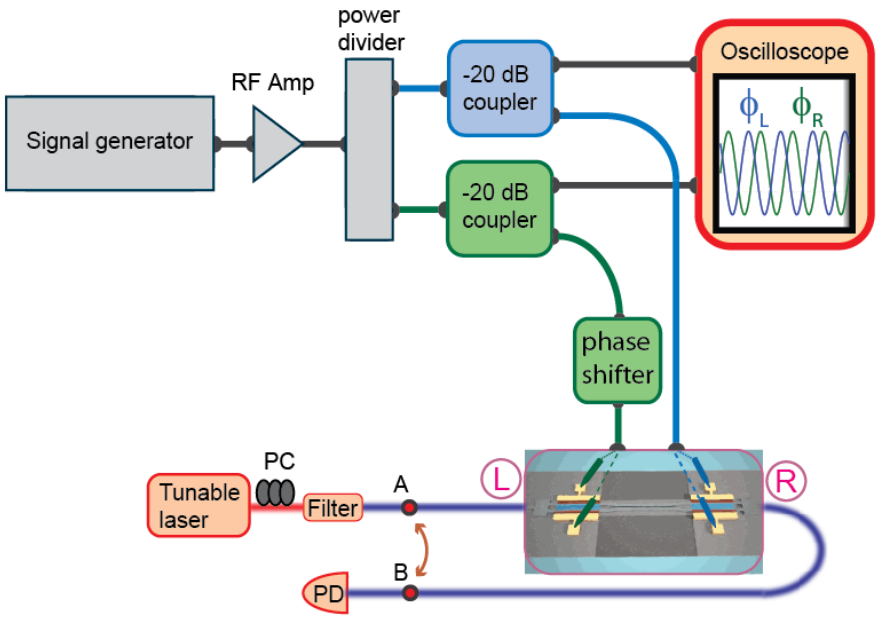

Fig. S6: **Experimental setup using an RF amplifier.** The RF signal coming out of the signal generator is amplified and splits into two arms. Signal in each arm is delivered to the right or the left modulator. A phase shifter is added on one of the RF arm.

References

1. Haus, H. & Huang, W. Coupled-mode theory. *Proceedings of the IEEE* **79**, 1505 –1518 (1991).

2. Little, B., Chu, S., Haus, H., Foresi, J. and Laine, J.-P. Microring resonator channel dropping filters. *J. of Lightwave Tech.* **15**, 998 –1005 (1997).

3. Fang, K., Yu, Z. & Fan, S. Photonic Aharonov-Bohm effect based on dynamic modulation. *Phys. Rev. Lett.* **108**, 153901 (2012).

4. Coldren, L. A. & Corzine, S. W. *Diode Lasers and Photonic Integrated Circuits* (Wiley, New York, 1995).